Multi-Hazard Seismic Risk Assessment for Tongatapu, Tonga

Timothy Mote[1], Karen Barnes[2], Caitlin Jay[1], Luke Johnstone[1], Jose Borrero[3], Minly So[4], Meg Ackerson[2], Kathy Franklin[1], Pranav Rawal[1], and Ed Rowe[1]

1. Arup, Sydney Australia

2. Arup, San Francisco USA

3. eCoast, Raglan New Zealand

4. Arup, Hong Kong

Abstract

To address risk and resilience to natural hazards in Tongatapu, Tonga a multi-hazard risk assessment was completed to inform planning and investments for the Government of Tonga. This paper presents the methodology and findings of the earthquake components of the multi-hazard risk assessment, particularly ground shaking, ground deformation, and tsunami inundation. Earthquake ground motions and permanent ground deformation were derived through a site-specific PSHA. A deterministic tsunami assessment was based on a range of tsunamigenic earthquakes occurring on the Kermadec Tonga Trench. A database was developed to capture characteristics and location of approximately 64,000 buildings, roads, water, and power assets across Tongatapu. Vulnerability curves were identified from literature or developed for the project for each of hazard and asset class pairs. Risk was quantified as financial loss through the integration of hazard, exposure, and vulnerability. The earthquake hazard risk is compared to other climate and natural hazards.

Keywords: multi-hazard risk assessment, Tonga, seismic, earthquake, tsunami, vulnerability

1 Introduction

Owing to its low relief most of the capital city of Nuku'alofa on the island on Tongatapu, Tonga is slightly more than 2.0m above current sea level. It is vulnerable to pluvial (surface) flooding as a result of heavy rainfall, including during cyclones, and coastal flooding from extreme sea levels, cyclone-induced storm surge, and tsunami inundation. Tongatapu is also at risk of damaging cyclones and earthquakes. Modelling of these hazards under the 2011 Pacific Catastrophe Risk Assessment and Financing Initiative (PCRAFI) project showed a 1% chance in any given year of moderate to heavy earthquake damage with estimated long-term average annual loss from earthquake equates to 4.4% of national GDP, with an extreme loss potentially threatening 90% of GDP across the country.

To effectively prioritise investment in infrastructure combined with other adaptation strategies such as changes in building policies, relocation or reclassification of urban areas, etc., the Government of Tonga through the Asian Development Bank (ADB) carried out a multi-hazard climate and disaster risk assessment for Tongatapu (ADB 2021). Hazards included pluvial flooding, coastal inundation, wind, seismic, and tsunami. Asset classes included buildings, roads, power, and water.

This paper presents the methodology and findings of the earthquake components of the multi-hazard climate and disaster risk assessment, particularly ground shaking, ground deformation, and tsunami inundation. Risk is represented as direct financial loss from the integration of hazard, exposure and vulnerability (Figure 1).

Figure 1: Risk = hazard x exposure x vulnerability.

2 Seismotectonic Background

Tonga is located on the boundary where the Pacific Plate subducts westerly underneath the Indo-Australian Plate along the Kermadec Tonga Trench (KTT) (Figure 2). Complex tectonic interactions and associated distribution of crustal stress throughout the plate boundaries (Bird, 2003) results in high seismic activity.

At the latitude of Tonga, the north-south trending KTT accommodates the majority of east to west plate convergence. Far to the south of Tonga, the KTT subduction zone extends to the North Island of New Zealand and transitions to a strike slip movement in the Alpine Fault. Approximately 800km north of Tonga, the KTT subduction zone curves westward to strike east-west. This change in geometry is accommodated by a number of transform and spreading boundaries transitioning into the New Hebrides Trench. Bird (2003) reports the KTT slipping at ~80mm/year in the south and increasing to ~220mm/year in the north.

Within the study area there have been 119 historical earthquakes with moment magnitude (Mw) >7, of which five were Mw >8. Although these all were of significant magnitude, they occurred at distance far enough away from Tongatapu to limit significant damage and fatalities.

There have been several tsunamigenic earthquakes in the Tonga region in recorded history (Okal et al., 2011), however none have caused destructive effects in Tongatapu. The most damaging event in recent history was the earthquake of 29 September 2009 near Samoa >700km to the north, which produced extreme tsunami heights of greater than 20m and 12m on the northern Tongan islands of Tafahi and Niuatoputapu, but negligible effects on Tongatapu (Fritz et al., 2011).

Despite its location close to the Kermadec Tonga Subduction Zone Trench, Nuku'alofa has experienced relatively little damage from earthquakes and tsunami during its history of settlement.

3 Hazard: Ground Motions

A probabilistic seismic hazard analysis was completed for Tongatapu based on the methodology of Cornell (1968). The probabilistic seismic hazard calculations were carried out using the Arup program *Oasys SISMIC* (Thomas et al., 2010). The analyses calculate the peak ground acceleration (PGA) and the uniform hazard response spectra (UHRS) for a given annual probability of exceedance (APE).

3.1 Earthquake Catalogue

An earthquake catalogue of 96,820 events was compiled for the region containing instrumental and historical records. Instrumental records from 1901 were compiled from the International Seismological Centre (ISC, 2020a), ISC EHB Bulletin (ISC, 2020b) and the ISC Global Instrumental Earthquake (GEM) Catalogue (ISC,2020c). Earthquake catalogue processing included magnitude scale conversion to Mw, foreshock/aftershock removal (declustering), and catalogue completeness.

3.2 Seismotectonic source model

Seismotectonic sources within 500km around the site comprised of the delineation and characterisation of areas based on the tectonic setting and spatial distribution of observed seismicity with depth. Sources included shallow areal source zones (0 to 35km deep), subduction intraslab areal zone sources (35 to 800km deep), and the KTT subduction interface fault (Figure 2). The KTT was modelled following the GEM Active Fault Database (Styron 2020).

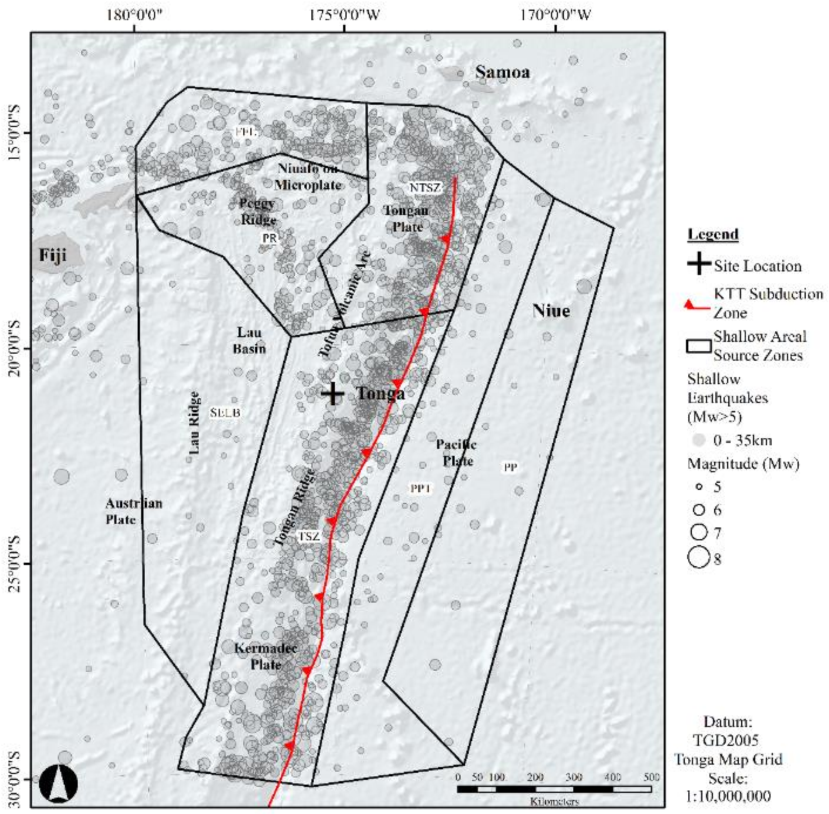

Figure 2: Shallow source zones with complete earthquake catalogue (Mw >5 and depth < 35km).

3.3 Ground Motion Predication Equations

There are limited strong motion recordings from the southern Pacific, and as such there are no specific Ground Motion Predication Equations (GMPE) for the southern Pacific region. GMPEs that consider strong motion recordings from subduction zone earthquakes in Japan (i.e. Zhao et al., 2006), have been shown by Ghasemi et al. (2016) to be appropriate for application in Papua New Guinea. Epistemic uncertainty was captured in a logic-tree. The following GMPEs were used for respective seismic source types:

Active shallow crustal sources: Zhao et al. (2006) and the Next Generation Attenuation-West2 (Abrahamson et al. 2014, Boore et al., 2014 Campbell et al., 2014 and Chiou et al., 2014)

Subduction zone sources: Zhao et al. (2006) and Abrahamson et al. (2016)

3.4 Site conditions

Tongatapu was formed by progressive uplift of carbonate deposits on the Australian Plate over-riding the Tonga subduction zone. The island has also received distal tuffaceous contributions as a result of volcanic action in the Tonga group.

Nuku'alofa is founded principally on a series of uplifted, recrystallised limestones blanketed by tuffs derived from nearby volcanic centres. Superficial Holocene fringing coral reefs and associated carbonate and organic-rich deposits occur in the coastal and lagoon areas. Holocene deposits have accumulated in beach, tidal-flat and lagoonal environments to form the northern coastal fringe, as well as the intertidal flats on the northwestern side of the island and the bottom sediments of Fanga'uta Lagoon.

Site conditions across Tongatapu were assessed using available geologic and geotechnical data and classified to the Site Sub-Soil Classes as defined in NZS1170.5 (2004) (Figure 3). The interpreted data included a microtremor geophysical survey ascertain shear wave velocity of Nuku'alofa geology (Shorten et al., 2001), Soil Map of Tonga (Manaaki Whenua Landcare Research 2020) and numerous geotechnical investigations in Tongatapu.

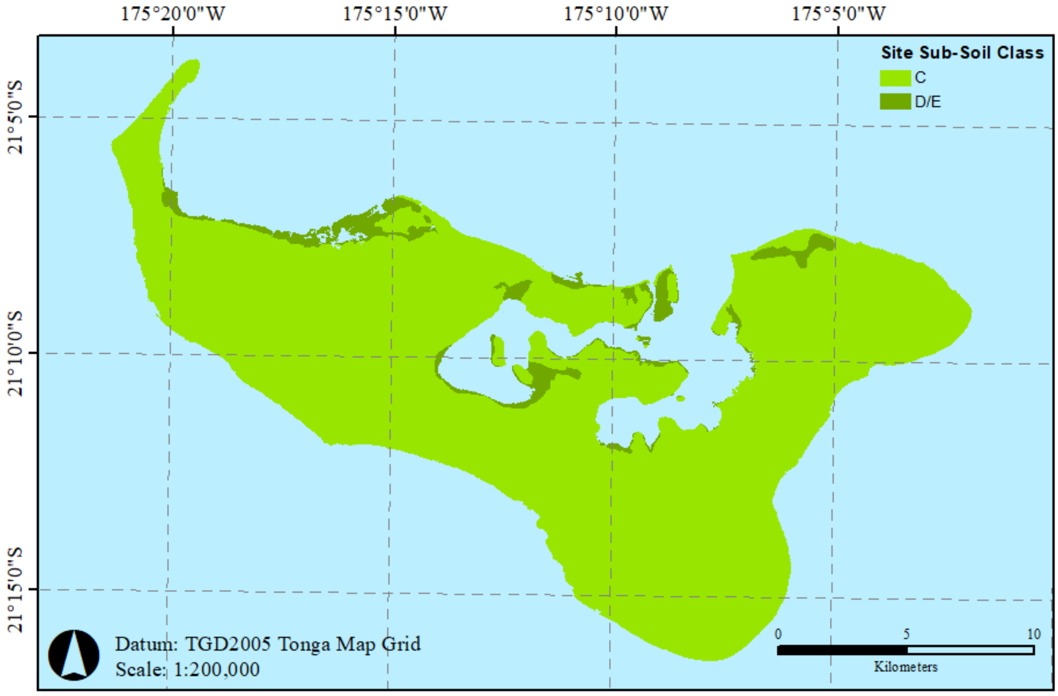

Figure 3: Tongatapu Site Sub-Soil Class map. Classified as per NZS1170.5 (2004)

3.5 Earthquake ground motion results

The results of the probabilistic seismic hazard analysis (PSHA) reports a peak ground acceleration (PGA) of 0.68g in bedrock (760m/s) for a 1/500 APE. The reported PGA results are consistent with recent studies from the Global Earthquake Model (Johnson et al., 2021) and USGS (Peterson et al., 2012), but report a 30% increase from the 2011 PCRAFI study (Rong et al., 2012).

The current Tonga National Building Code, following NZS1107.5, uses a "Z" value of 0.4g, equivalent to PGA in rock for 1/500 APE, for design. The Tonga National Building Code is under recommendation to increase "Z" to 0.70g in line with this and other studies.

3.6 Magnitude Distance Deaggregation

The magnitude and distance deaggregation shows a significant contribution to of the hazard is driven by M 7.75-8.00 earthquakes from the KTT subduction zone ~60km to the east (Figure 4).

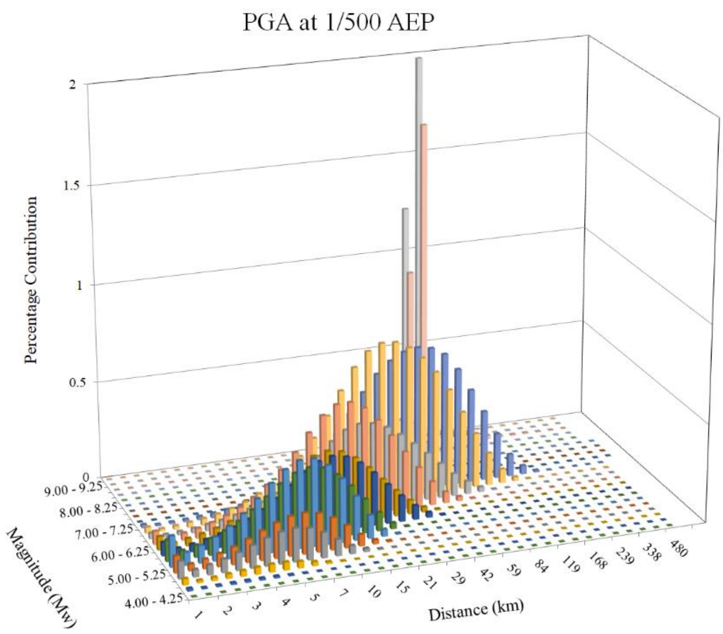

Figure 4: Magnitude distance deaggregation of hazard for PGA with a 1/500 APE.

4 Hazard: Ground Deformation

Though seismic shaking drives the loss for buildings and other structures, permanent ground deformation (PGD) drives loss to linear assets, such as roads and water pipelines.

An estimation of PGD was developed based on liquefaction susceptibility across Tongatapu using a methodology by the American Lifelines Alliance (ALA, 2005) using liquefaction susceptibility, PGA and design magnitude. Ground deformation from fault rupture from active faulting was not considered a credible hazard across Tongatapu.

4.1 Liquefaction susceptibility mapping

Liquefaction susceptibility was classified across the island based on available geologic and limited geotechnical information consistent with Youd and Perkins (1978) (Figure 5). Estuarine and lagoon deposits were assigned a High liquefaction susceptibility and the Nuku’alofa sandy loam assigned a Moderate susceptibility. All other areas of the island were classified as having Low liquefaction susceptibility.

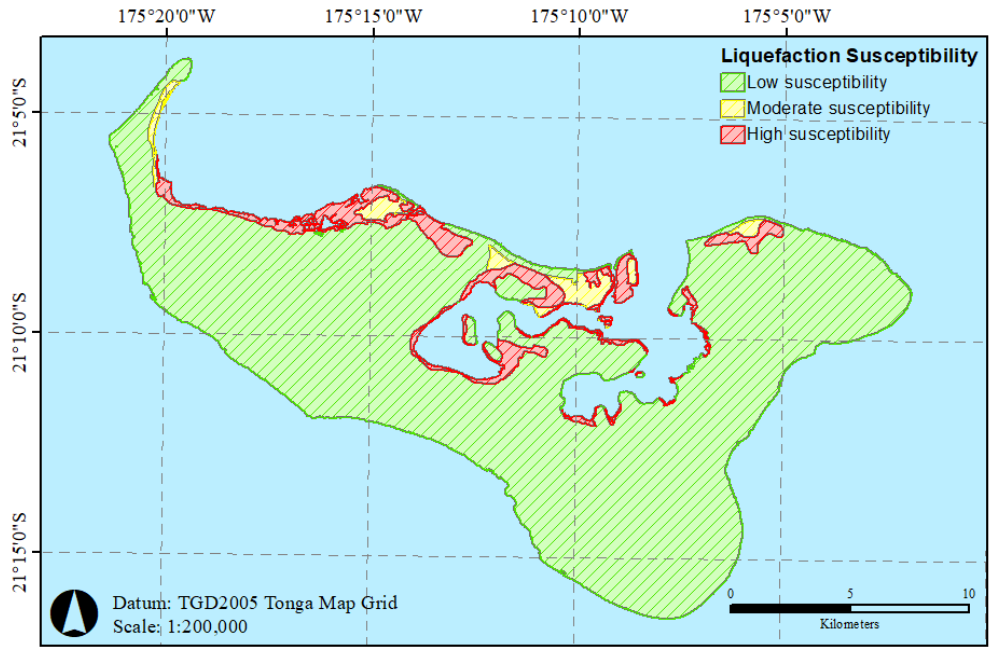

Figure 5: Tongatapu liquefaction susceptibility map.

4.2 Probability of liquefaction

The probability of liquefaction for the susceptibility zones (refer to Figure 5) were estimated at various APE using the PGA results and a scenario Mw 7.75-8.00 earthquake from the magnitude-distance deaggregation (Figure 4). Groundwater was assumed to be within 1m of the surface across the island. The results in Table 1 show High liquefaction susceptibility zones are estimated to have almost certain liquefaction from ground PGA motions at 1/500 and 1/2500 APE.

Table 1: Probability of liquefaction in susceptibility zones for select Annual Probability of Exceedance.

Annual Probability of Exceedance	Low	Moderate	High
1/100	7%	22%	57%
1/500	18%	48%	100%
1/2500	37%	92%	100%

5 Hazard: Tsunami

A deterministic assessment of tsunami inundation was conducted based on a range of subduction zone thrust earthquake sources occurring on the Tonga Trench using the ComMIT model (Borrero et al., 2021). A total of 10 KTT earthquake rupture scenarios were tested with magnitudes (Mw) of 9.0, 8.7 and 8.3 with variation in the source location and/or slip distribution within each magnitude. Each scenario was run at present day mean sea level (MSL) and for sea level rise (SLR) scenarios of 1.0, 2.0, 4.0 and 6.0m above present day MSL.

5.1 Results

Due to its low-lying topography, the northern coast of Tongatapu is most vulnerable to tsunami inundation. Particularly vulnerable are the villages on the north-facing portion of the island to the east of Nuku'alofa (across the entrance of Fanga'uta Lagoon). These areas are shown to be inundated in scenarios when Nuku'alofa itself is relatively unaffected. The Mw 9.0 Central source scenario has a maximum amplitude of 6.2m and results in the largest area inundated. (Figure 6).

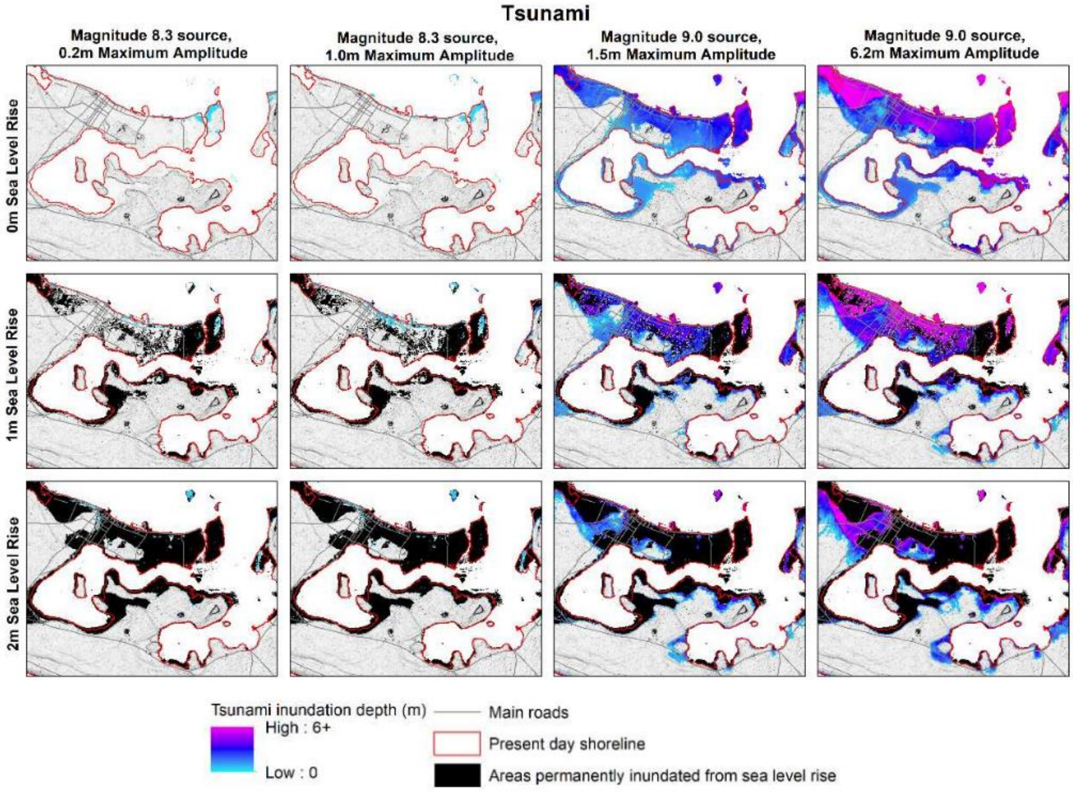

Figure 6: Tsunami inundation results considering various sea level raise scenarios and deterministic tsunami scenarios.

6 Exposure Data Development and Assessment

Extensive data gathering, collection and validation was completed to produce an asset database. This database captures attributes, characteristics, and the location of approximately 64,000 buildings, roads, water assets, and power assets across Tongatapu.

6.1 Remote data collection

The data compiled from existing sources (e.g. PCRAFI and Open Street Map) provided a baseline of assets and their attributes, however further information was required to be able to have a more comprehensive understanding of the assets. As such, additional remote data collection was undertaken using the Post-TC Gita Aerial Imagery and Google Street View.

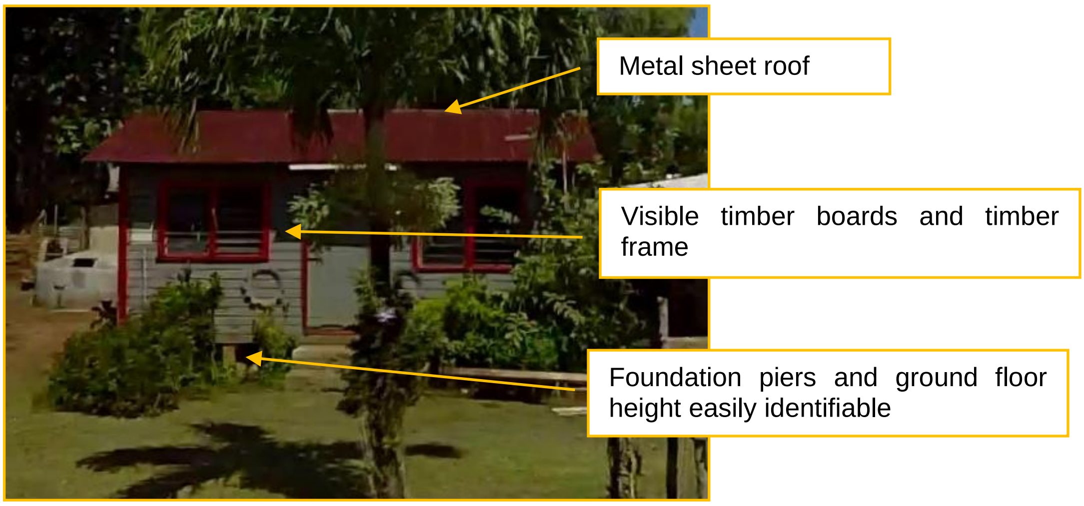

Figure 7: Example of building assessed during the Google Street View remote survey.

6.2 Field mission

Data was collected in-country during an exposure data collection mission. At the beginning of each phase of the mission, a series of interactive training workshops were held to introduce the iPads, the Survey123 survey forms, and how to answer the questions within the survey forms.

6.3 Machine learning imputation

Following completion of the above steps there were some asset attributes missing, notably 50% of buildings with plan area greater than 20m^2 had no attributes. A probabilistic method was used to statistically assign these missing attributes. A dataset containing the most common value (i.e., median) for each attribute for each building from 100 samples was created to impute into the asset database. The validation compared imputed data against observed data and assessed that the overall distributions of variables were similar.

7 Vulnerability

Vulnerability to seismic hazards and tsunami were reviewed for all asset classes. Table 2 and Table 3, present the vulnerability of fragility functions used for each asset-hazard pair.

7.1 Seismic Ground Shaking and Ground Deformation

Table 2: Summary of methodology used to assess vulnerability to seismic hazards for each asset.

Assets		Seismic
Buildings		Adopted from literature with minor modification, from PCRAFI study, Bazzurro (Bazzurro, 2015). Based on Federated States of Micronesia, Marshall Islands, Samoa, Tonga, and Vanuatu.
Roads (paved, unpaved, and informal tracks)		Adopted from literature without modification, US FEMA (FEMA, 2020). Based on data from the US.
Power	Power distribution	Adopted from literature without modification, US FEMA (FEMA, 2020). Based on data from the US. Ground- mounted transformers: Adopted from literature without modification, US FEMA (FEMA, 2020). Based on data from the US.
	Power station	Adopted from literature without modification, US FEMA (FEMA, 2020). Based on data from the US.
	Wind farm - auxiliary equipment	For equipment and machinery curves from PV panels were adopted.

		For the building housing this equipment curves from the steel frame typology for buildings was used.
	Solar farms (PV Panels)	PV Panels - Adopted without modifications from Miyamoto International Inc. Based on data from the US.
Water	Elevated water tanks	Adopted without modification from ALA (American Lifelines Alliance, 2001). Based on data from the US.
	At grade water tanks	Adopted without modification from ALA (American Lifelines Alliance, 2001). Based on data from the US.
	Buried pipelines	Adopted without modification from ALA (American Lifelines Alliance, 2001). Based on data from the US.
	Pumps and wells	Adopted without modification from Hazus (FEMA, 2020). Based on data from the US.

7.2 Tsunami

Table 3: Summary of methodology used to assess vulnerability to tsunami for each asset.

Assets		Tsunami
Buildings	Structural system	Adopted without modification from FEMA Hazus (FEMA, 2017).
	Building contents	Arup – developed from component-level building model. Based on housing data from Tonga.
Roads (paved, unpaved, and informal tracks)		Adopted without modification from Horspool & Fraser (Horspool & Fraser, 2016). Based on Post-tsunami damage reports from Samoa, Andaman Islands, Chile, Japan; expert judgment.
Power	Power distribution	Adopted without modification from Horspool & Fraser (Horspool & Fraser, 2016). Based on Post-tsunami damage reports from Samoa, Andaman Islands, Chile, Japan; expert judgment. Transformers will use the same fragility curves used in flood.
	Power station	Adopted without modification from Horspool & Fraser (Horspool & Fraser, 2016). Based on Post-tsunami damage reports from Samoa, Andaman Islands, Chile, Japan; expert judgment.
	Wind farm - auxiliary equipment	Indoor auxiliary equipment covered by the same curves used for steel Structure vulnerability curve for building and flood vulnerability of a specialised building.
	Solar farms (PV Panels)	Adopted without modification from Horspool and Fraser (Horspool & Fraser, 2016) based on Post-tsunami damage reports from Samoa, Andaman Islands, Chile, Japan; expert judgment.
	At grade water tanks	Adopted without modification from Hatayama (Hatayama, 2015). Based on data from Japan.
	Buried pipelines	Deemed rugged and not vulnerable to hazard.
	Pumps and wells	Develop by Arup – developed from analysis of assets, literature review (Horspool et al. (Horspool & Fraser, 2016)), workshops, and expert judgment.

8 Risk Assessment

The risk assessment was completed at an asset level using the Monte Carlo method. The hazard intensity (e.g. ground shaking) was sampled at each asset and then the level of damage the asset experiences was simulated based on the vulnerability or fragility curve for that asset/hazard combination. The cost associated with repairing the damage or replacing the asset if it were deemed a total loss was simulated based on information collected from government stakeholders and local engineers. This was repeated many times for each asset for each hazard scenario (e.g. each APE) and loss statistics were aggregated to the town and island level.

8.1 Seismic Risk Results

The average losses for each modelled earthquake event and the average annual loss (AAL) are approximately 1% of the total asset value of buildings, roads, water infrastructure, and power infrastructure on Tongatapu. These losses are distributed across Tongatapu, especially in the lower annual probability of exceedance events. Figure 8 highlights the significant damage to buildings experienced across Tongatapu in the event of a large seismic event – seen in the yellow and orange colours covering the island in the 1/500 APE event. For the 1/2500 APE event, the relative losses exceed 100% due to extra costs associated with the demolition of damaged buildings before they can be rebuilt.

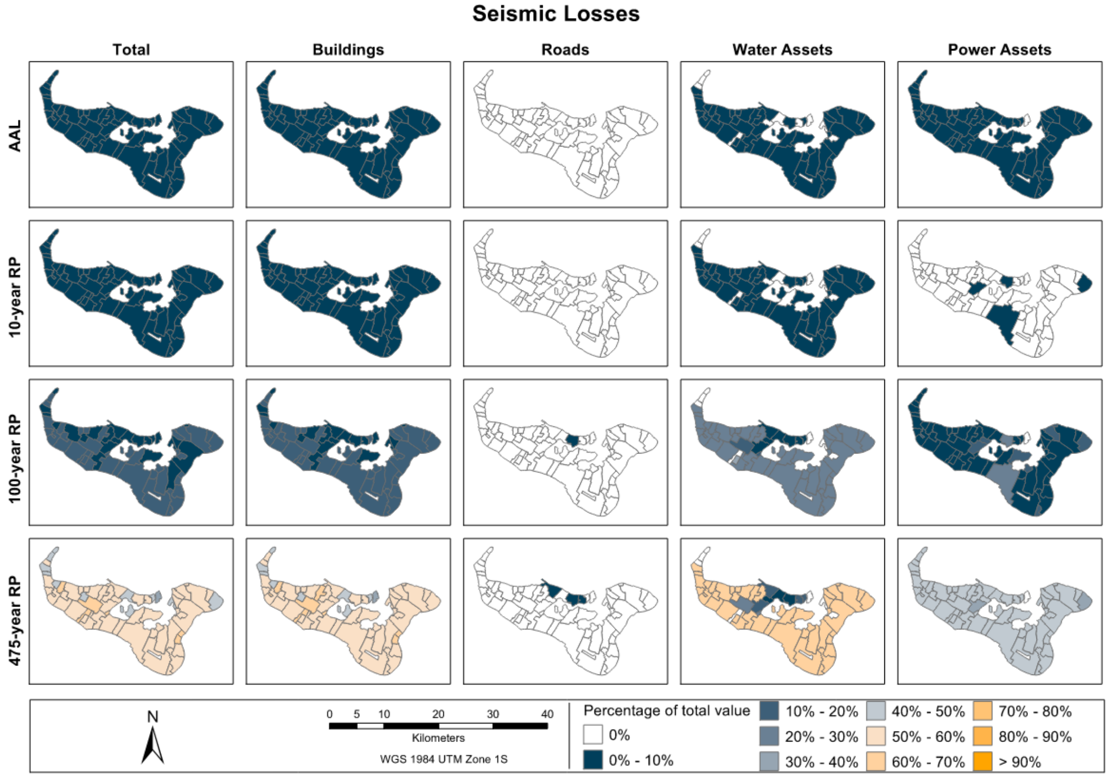

Figure 8: Seismic losses summed across all assets, presented as AAL in terms of percentage loss. Scenario losses also provided for the 1/10, 1/100, and 1/500 APE.

8.2 Tsunami

The losses from tsunami show a direct relationship between maximum offshore tsunami amplitude and damage. Similar to the inundation flooding hazards, buildings contribute most to the overall loss, owing to their significant total value.

8.3 Multi-hazard considerations

The climate and multi-hazard disaster risk assessment also considered pluvial flooding, coastal inundation, and wind through a probabilistic risk assessment as presented above for seismic. Sea-level rise was expressed as permanent loss to assets that were permanently inundated.

Table 4 shows the percent loss vs total asset value considering a number of hazard and sea level rise scenarios.

Table 4: Multi-hazard comparisons

Hazard or SLR Scenario	Percent Loss vs Total Asset Value
Pluvial Flooding (200-yr RP)	7%
Coastal Inundation (200-yr RP)	0%
Wind (200-yr RP)	3%
Seismic (200-yr RP)	19%
Tsunami (M8.3, 1.0m Amplitude)	0%
Sea Level Rise 0.5m - Permanent Loss	6%

Sea Level Rise 1.0m - Permanent Loss	25%
Sea Level Rise 2.0m - Permanent Loss	49%

9 Conclusions

The key findings of the earthquake components of the climate and multi-hazard disaster risk assessment are:

- The PSHA reports higher seismic hazard than in the current Tongan National Building Code. This supports current recommendations to increase the seismic design levels in the Building Code.
- The AAL from ground shaking and liquefaction are approximately 1% of the total asset value of buildings, roads, water infrastructure, and power infrastructure on Tongatapu.
- For the 1/2500 APE event, the relative losses exceed 100% of current asset value due to extra costs associated with the demolition of damaged buildings before they can be rebuilt.
- Tsunami with the highest maximum amplitude considered in the risk assessment (Mw9.0 earthquake along the KTT with a 6.2m offshore wave amplitude) reported losses to 10% of total asset value on Tongatapu. Losses were concentrated in Nuku'alofa and the towns surrounding the lagoon.
- Building losses drive the overall loss across all hazards on Tongatapu as they make up the majority of the total asset value on Tongatapu. The losses from water and power assets are comparatively low, however the service disruption caused by damage may have major customer impact which is not captured in these financial metrics. The highest losses occur in the Nuku'alofa area due to the concentration and high value of exposed assets.
- With rarer hazard events, seismic hazards are associated with larger relative losses (as a percentage of the total asset value) than other hazards.
- A 1/200 APE seismic event will result in damage equivalent to a permanent loss from ~1.0m of sea level rise.

10 Acknowledgements

The authors wish to thank two AEES reviewers for their constructive comments.

© Asian Development Bank. 2021. Multi Hazard Disaster Risk Assessment, Tongatapu - Risk Assessment Summary Report. Used with permission.

The Asian Development Bank is the sole owner of the copyright in ADB Contribution developed or contributed for this Work, and has granted permission to the AEES to use said ADB-copyrighted Contribution for this Work, and to make the Contribution available under an open access license.

The views expressed in this publication are those of the authors and do not necessarily reflect the views and policies of the Asian Development Bank (ADB) or its Board of Governors or the governments they represent. ADB does not guarantee the accuracy of the data included in this publication and accepts no responsibility for any consequence of their use.

By making any designation of or reference to a particular territory or geographic area, or by using the term "country" in this document, ADB does not intend to make any judgments as to the legal or other status of any territory or area.

11 References

Abrahamson, N., Silva, W., and Kamai, R. (2014). Summary of the ASK14 Ground-Motion Relation for Active Crustal Regions. Earthquake Spectra. (NGA-West2 ASK14)

Abrahamson, N., Gregor, N. & Addo, K. (2016). *BC Hydro ground motion prediction equations for subduction earthquakes*. Earthquake Spectra, 32(1), 23-44.

American Lifelines Alliance. (2001). Seismic Fragility Formulations for Water Systems: Part 1 - Guideline. ALA, FEMA, and ASCE.

Asian Development Bank. (2021). Multi Hazard Disaster Risk Assessment, Tongatapu - Risk Assessment Summary Report. https://www.adb.org/sites/default/files/project-documents/50028/50028-001-tacr-en_19.pdf.

Bazzurro, P. (2015). Retrofit Measures and Damage Functions for Residential and Public Buildings in Federated States of Micronesia, Marshall Islands, Samoa, Tonga and Vanuatu.

Bird, P., 2003, An updated digital model of plate boundaries. Geochemistry Geophysics Geosystems, v 4, p. 1–52.

Boore, D. M., Stewart, J. P., Seyhan, E., and Atkinson, G. M. (2014). NGA-West2 equations for predicting PGA, PGV, and 5% damped PSA for shallow crustal earthquakes. Earthquake Spectra, 30(3), 1057-1085. (NGA-West2 BSSA14)

Borrero, J., Greer, D., McIntosh, R. and Damlamian, H. (2021) Tsunami Hazard Assessment for Tongatapu, Tonga, Proceedings Australasian Coasts & Ports 2021 Conference. Campbell, K. W., and Bozorgnia, Y. (2014). NGA-West2 Ground Motion Model for the Average Horizontal Components of PGA, PGV, and 5%-Damped Linear Acceleration Response Spectra. Earthquake Spectra. (NGA-West2 CB14)

Chiou, B. S. J., and Youngs, R. R. (2014). Update of the Chiou and Youngs NGA model for the average horizontal component of peak ground motion and response spectra. Earthquake Spectra. (NGA-West2 CY14)

Cornell, C.A. (1968). Engineering seismic risk analysis. Bulletin of the Seismological Society of America, 58, 1583-1606.

FEMA. (2017). Hazus Tsunami Model Technical Guidance. Herndon, VA, USA: FEMA US Department of Homeland Security.

FEMA. (2020). Hazus Earthquake Model Technical Manual 4.2. FEMA.

Fritz, H.M., Borrero, J.C., Synolakis, C.E., Okal, E.A., Weiss, R., Titov, V., Jaffee, B., Foteinis, S., Lynett, P., Chan, I., and Liu, P.L-F (2011) Insights on the 2009 South Pacific Tsunami in Samoa and Tonga from Field Surveys and Numerical Simulations, Earth Sci. Revs., 107, 66–75.

Ghasemi, H., McKee, C., Leonard, M., Cummins, P., Moihoi, M., Spiro, S., Taranu, F. and Buri, E., 2016. Probabilistic seismic hazard map of Papua New Guinea. Natural Hazards, 81(2), pp.1003-1025.

Hatayama, K. (2015). Damage to Oil Storage Tanks from the 2011 Mw 9.0 Tohoku-Oki Tsunami. Earthquake Spectra, 31(2).

Horspool, N. A., & Fraser, S. (2016). An analysis of tsunami impacts to lifelines. GNS Science Report 2016/22.

International Seismological Centre (2020a), On-line Bulletin, https://doi.org/10.31905/D808B830.

International Seismological Centre (2020b), ISC-EHB dataset, https://doi.org/10.31905/PY08W6S3.

International Seismological Centre (2020c), ISC-GEM Earthquake Catalogue, https://doi.org/10.31905/d808b825.

Johnson, K.L., Pagani, M. and Styron, R.H., 2021. PSHA of the southern Pacific Islands. Geophysical Journal International, 224(3), pp.2149-2172.

Manaaki Whenua Landcare Research. (n.d.)., (2020). Pacific Soils Portal Tonga. https://tonga-psp.landcareresearch.co.nz/maps/. Accessed 2020.

NZS 1170.5 New Zealand Standard Structural Design Actions. Part 5: Earthquake Actions - New Zealand (2004).

Okal, E.A., Borreo, J., and Synolakis, C.E., (2004). The earthquake and tsunami of 1865 November 17—Evidence for far-field tsunami hazard from Tonga. Geophysical Journal International, v. 157, p. 164–174.

Petersen, M.D., Harmsen, S.C., Rukstales, K.S., Mueller, C.S., McNamara, D.E., Luco, Nicolas, and Walling, M., (2012). Seismic hazard of American Samoa and neighboring South Pacific Islands—Methods, data, parameters, and results. U.S. Geological Survey Open-File Report 2012–1087, 98 p.

Rong, Y., Park, J., Duggan, D., Mahdyiar, M. and Bazzurro, P., 2012. Probabilistic seismic hazard assessment for Pacific Island Countries. In 15th World Conference on Earthquake Engineering.

Styron, S. and Pagani, M., (2020) The GEM Global Active Faults Database. Earthquake Spectra, vol. 36, no. 1_suppl, Oct. 2020, pp. 160–180, doi:10.1177/8755293020944182.

Thomas, P., Wong, I. and Abrahamson, N., 2010. Verification of probabilistic seismic hazard analysis computer programs. PEER-2010/106, Pacific Earthquake Engineering Research Center, University of California, Berkeley, 2010-05, PDF (4.88 MB)(400/P33/2010-106). Available online: http://peer. berkeley. edu/publications/peer_reports/reports_2010/web_PEER_10106_THOMASetal. pdf.

Youd, T., L., & Perkins, D., M., (1978). Mapping liquefaction-induced ground failure potential. Journal of the Soil Mechanics and Foundations Division, 104(4), 433-446.

Zhao, J. X., Zhang, J., Asano, A., Ohno, Y., Oouchi, T., Takahashi, T., Ogawa, H., Irikura, K., Thio, H. K., Somerville, P. G. & Fukushima, Y., (2006). Attenuation relations of strong ground motion in Japan using site classification based on predominant period. Bulletin of the Seismological Society of America, Vol. 96, No. 3, pp. 898–913.